

An optical detection system for biomedical photoacoustic imaging

Beard PC* and Mills TN

Department of Medical Physics and Bioengineering, University College London, Shropshire House,
11-20 Capper Street, London WC1E 6JA, UK

ABSTRACT

An all-optical system for the detection of photoacoustic transients is under development for photoacoustic imaging applications. The sensing mechanism is based upon the detection of acoustically-induced variations in the optical thickness of a Fabry Perot polymer film interferometer and provides an alternative to piezoelectric based detection methods. A key advantage is that the sensing geometry is defined by the area of the polymer sensing film that is optically addressed. This offers the prospect of obtaining sufficiently small element sizes and interelement spacing to employ the synthetic focussing techniques of phased arrays for image reconstruction. The optical nature of detection also allows for a transparent sensor head through which the excitation laser pulses can be transmitted for backward-mode photoacoustic imaging. Preliminary work has shown that the detection sensitivity ($<10\text{kPa}$ - without signal averaging) and bandwidth (30MHz) are comparable to wideband piezoelectric PVDF ultrasound transducers with the prospect of achieving substantially smaller element sizes ($<35\mu\text{m}$).

Keywords: Photoacoustic imaging, ultrasound array, biomedical, Fabry Perot sensor.

1. INTRODUCTION

The use of photoacoustic imaging techniques for visualising the internal structure of soft biological tissues is currently exciting much interest. This new approach to medical imaging relies upon irradiating the tissue with low energy, nanosecond pulses of laser light at a wavelength in the visible or near-infrared (NIR). Broadband ($\sim 30\text{MHz}$) ultrasonic thermoelastic waves are excited throughout the irradiated volume at optically absorbing subsurface features and propagate to the surface of the tissue. The photoacoustic signals are then detected and spatially resolved to reconstruct a 3D image of the internal tissue structure in much the same way that volumetric images are formed in conventional medical ultrasound imaging using tomographic, line-of-sight or phased array methods. A key advantage of the technique is that it exploits the strong optical contrast of tissues enabling differentiation of anatomical features that would be indistinguishable using other radiological modalities. A broad range of potential applications have emerged including detection of breast^{1,2}, skin and oral cancers³ and vascular applications such as imaging superficial blood vessels^{4,5} and the characterisation of arterial tissues⁶.

Detection of the photoacoustic signals can be achieved, as with conventional ultrasound imaging, using piezoelectric transducers. There are however substantial difficulties involved in fabricating high density 2D piezoelectric arrays with sufficiently small element sizes and interelement spacings. This is particularly so for phased arrays where, for optimum lateral spatial resolution, a near-omnidirectional element response is required necessitating an element size that is small in comparison to the acoustic wavelength. Sub- $50\mu\text{m}$ element sizes are required for an isotropic response at 10 MHz, for example. To achieve this with adequate wideband detection sensitivity ($<1\text{kPa}$) using piezoelectric transducers represents a major challenge. A further difficulty lies in implementing the so-called backward-mode of photoacoustic imaging where the acoustic signals are detected on the same side of the tissue that the excitation laser pulses are delivered to. This requires a transparent detector head through which the excitation laser pulses can be transmitted.

* Correspondence to P Beard, Dept of Medical Physics, UCL, Shropshire House, 11-20 Capper Street, London WC1E 6JA, UK, EMail: pbeard@medphys.ucl.ac.uk

A solution may lie in optical detection methods in which the acoustic field distribution is mapped on to an optical field. These offer the prospect of a transparent sensor head and, by transferring the spatial discretisation of the detection process from the acoustic detection plane to a remotely located array of optical detectors, the possibility of smaller effective element sizes and interelement spacings than can be achieved with piezoelectric arrays. Several approaches have been investigated. The detection of acoustically-induced changes of optical reflectance at a glass-liquid interface⁷ has been demonstrated for single point photoacoustic measurement of the optical properties of tissues⁸ and 2D photoacoustic imaging⁹. Interferometric detection of acoustically-induced displacements across the surface of a pellicle¹⁰ and the detection of changes in the optical thickness of a multilayer dielectric stack Fabry Perot (F-P) interferometer¹¹ have also been investigated for ultrasound imaging and field mapping. The use of a polymer film Fabry Perot sensing interferometer as an ultrasound sensor¹² has also been studied by ourselves in the form of an all-optical photoacoustic probe¹³ and a miniature ultrasonic hydrophone¹⁴. In this paper, we examine the feasibility of extending this approach to the development of a 2D optical ultrasound array for photoacoustic imaging applications. Section 1 describes the basic principles of the concept. Section 2 discusses the acoustic characteristics of F-P polymer film transducers and their relevance to photoacoustic imaging. Section 3 describes the fabrication and preliminary characterisation of a prototype sensing head.

2. PROPOSED PHOTOACOUSTIC IMAGING SYSTEM

An example of a photoacoustic imaging scheme using a FP polymer film sensor is illustrated in figure 1. Nanosecond excitation laser pulses are transmitted through the sensor head and into the target generating photoacoustic contributions from each point in the diffusely irradiated tissue volume - for the purposes of illustration, a single cylindrical absorbing subsurface “feature” from which a photoacoustic signals emanates is depicted in figure 1

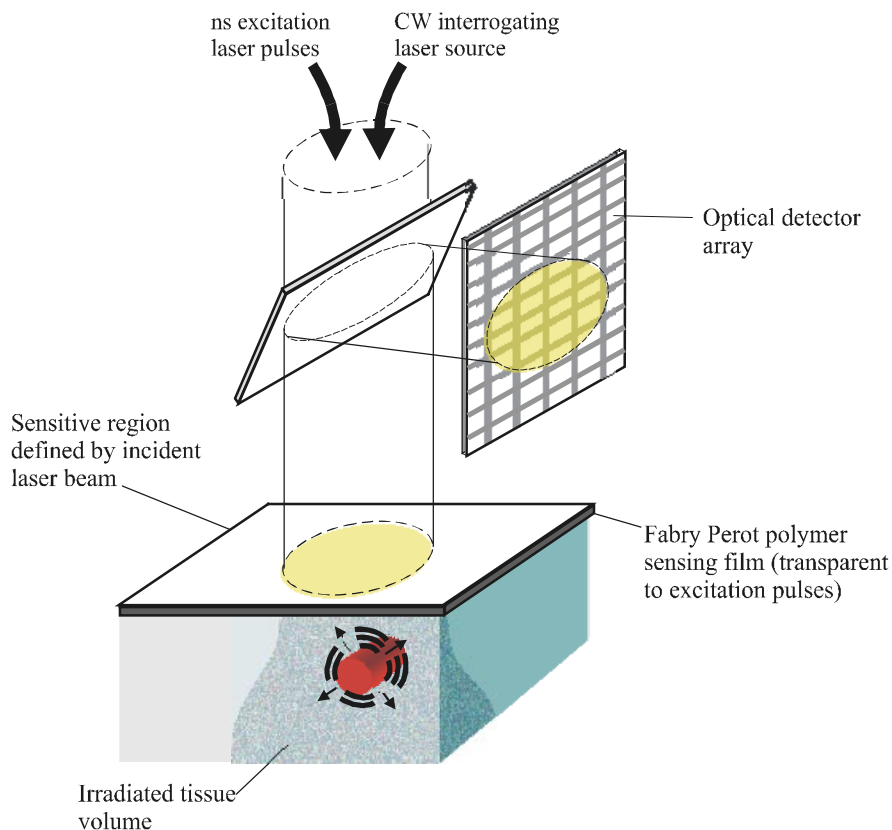


Figure 1 Schematic of proposed photoacoustic imaging system

The photoacoustic signals are detected by the sensor head which is placed in acoustic contact with the tissue. The sensing element itself comprises an acoustically thin ($\sim 50\mu\text{m}$) polymer film. When illuminated by the output of a cw interrogating laser source (aligned coaxially with the pulsed excitation beam), the film acts as a F-P interferometer, the mirrors of which are formed by the deposition of wavelength selective dielectric coatings. These are designed to be reflective at the cw interrogating laser wavelength but transparent at the wavelength of the excitation laser pulse. An incident photoacoustic signal modulates the optical thickness of the polymer film resulting in a modulation of the reflected light. By directing the reflected optical beam on to a 2-D detector array (e.g. a CCD or photodiode array), a representation of the incident acoustic field across the sensing film can be obtained. In its simplest form it is a 1-1 mapping so, to a first approximation, the effective acoustic element size and interelement spacing is simply that of the detector array. The output of the detector array can then be multiplexed and processed in much the same way that the output of a conventional piezoelectric ultrasound array is used to reconstruct an image. This approach fulfills the requirement for a transparent sensor head and, given the good detection sensitivities previously reported¹⁴ and the advantages of optical mapping, the prospect of overcoming the element size-sensitivity limitations of piezoelectric methods.

3. F-P POLYMER FILM TRANSDUCER PRINCIPLES AND CHARACTERISTICS

3.1 Principles of operation

The transduction mechanism of a F-P ultrasound transducer comprises two processes. Firstly, assuming the elastic limits of the polymer sensing film are not exceeded, external acoustic pressure is linearly converted to a change in the optical thickness of the film (fig 2(a)). Secondly, the resulting optical phase shift is converted to an intensity (figure 2(b)) modulation through the intensity-phase transfer function of the interferometer. The latter is not strictly linear although by setting the phase bias appropriately (see figure 2(b)) by tuning the laser wavelength, small phase shifts can be detected with acceptable linearity.

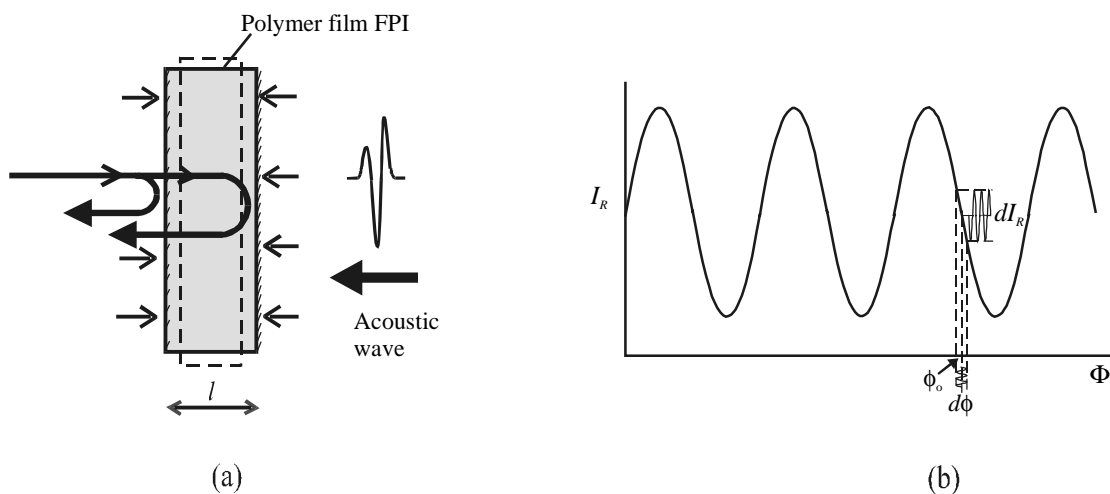


Figure 2 (a) *FP polymer film ultrasound sensor and (b) low finesse FP interferometer transfer function*

Note that figure 2(b) shows the raised cosine transfer function characteristic of a two beam interferometer. In a F-P cavity, this occurs when the reflectivities of the cavity mirrors are small ($<10\%$) or there is significant optical absorption in the mirrors as is the case with aluminum reflective coatings. In both cases the contribution of multiple reflections to the reflected fringe system can be neglected and the interferometer becomes one of low finesse. Whilst higher sensitivity can be achieved using high reflectivity low absorption dielectric mirrors to create a high finesse F-P

cavity, there are several important practical advantages to the low finesse configuration. It offers reasonable detection sensitivity, comparable to PVDF transducers^{12,14} and a useful linear phase range with the detection of phase shifts up to 0.8 rad with a linearity of better than 10%. An optimum fringe visibility close to unity can be achieved with a relatively wide range mirror reflectivities reducing the requirements of the optical coating process. Furthermore, the wavelength tuning range and stability requirements for the laser source are relatively relaxed compared to those for a high finesse cavity.

3.2 Sensitivity

To formalise the description of sensitivity it is helpful to define figures of merit for each transduction process. The *phase sensitivity* I_s represents the slope efficiency of the conversion of optical phase $d\phi$ to intensity output dI_R and is defined as the optical power modulation per unit phase shift ($\mu\text{W}/\text{rad}$) at the phase bias ϕ_o

$$I_s = \left[\frac{dI_r}{d\phi} \right]_{\phi_o} \quad (1)$$

Thus I_s is dependent upon the incident laser power and the reflectivity and absorbance characteristics of the reflective coatings that form the mirrors of the interferometer¹². With knowledge of the detector noise floor, I_s can be used to determine the phase resolution of the interferometer - mrad phase noise floors over a 25MHz measurement bandwidth with low finesse cavities have been reported¹².

The *acoustic phase sensitivity* A_s represents the conversion of external acoustic pressure to an optical phase shift. It is defined as magnitude of the optical phase shift produced per unit acoustic pressure (rad/MPa). It is thus a measure of the acoustically-induced change in optical thickness of the sensing film - the change in both physical thickness and refractive index and is dependent on the elastic and photoelastic properties of the cavity. It is given by

$$A_s = \frac{d\phi}{dP} = \frac{4\pi nl}{\lambda} \frac{1}{E} \left(1 + \frac{n^2 p \sigma}{2} \right) |P_l(k)| \quad (2)$$

where n is the refractive index, l is the thickness of the film, λ the laser wavelength, E the Young's modulus, p the photoelastic constant, σ Poisson's ratio. k is the acoustic wavenumber, $k=2\pi/\lambda_a$ where λ_a is the acoustic wavelength.

$P_l(k)$ is a frequency-dependent modifying term (discussed further in section 3.3) representing the net stress integrated across the thickness of the sensing film and is dependent upon the acoustic properties of the film, the backing material and the surrounding media (usually water). In the low frequency limit where $\lambda_a \gg l$, assuming the acoustic impedance mismatch between the sensing film and the surrounding fluid is small, $|P(k)|$ is dominated by the acoustic properties of the backing material. At low frequencies, $|P(k)|=0$ for a compliant backing such as air, $|P(k)|\sim 1$ for a backing of similar acoustic impedance such as water or a polymer and $|P(k)|\sim 2$ for a rigid backing such as glass¹². In this paper, the low frequency limit is implied when discussing acoustic phase sensitivity for a particular backing configuration.

The acoustic phase sensitivity enables (with knowledge of the form of the ITF) the acoustic pressure range over which the sensor is linear to be estimated and comparisons to be made between the intrinsic sensitivity of different sensing film materials, thicknesses and backing configurations. Typical values for A_s for 50 μm thick water-backed polymer films at 850nm are 0.1 rad/MPa for PET¹² and 0.075rad/MPa for Parylene¹⁴. For a low finesse cavity, this gives an upper limit of linear (<10%) detection of 10MPa and a dynamic range of 60dB.

The product of I_s and A_s gives the *overall sensitivity*. In principle, this could be optimised through A_s by selecting a polymer with appropriately high values of p and E . In practice, this is problematic due to the paucity of data available in the literature for these parameters at ultrasonic frequencies. Additionally, the selection of the polymer film tends to be dominated more by considerations of uniformity of thickness, surface finish and optical clarity than its mechanical/elastic properties. To optimise sensitivity it is more fruitful to consider the detector noise floor and the characteristics of the interferometer transfer function.

With a wideband (tens of MHz) silicon photodiode-transimpedance amplifier detector configuration, the output system noise tends to be dominated by a combination of the amplifier input noise voltage and the shot noise due to the photocurrent arising from the (large) dc interferometer output level I_R . 0.05 μW noise-equivalent powers are typical

although there is the potential for some improvement on this by reducing the amplifier input noise voltage. Greater scope for improving sensitivity lies in optimising the interferometer transfer function. For a low finesse configuration, it is desirable to design for a fringe visibility of unity and operate at a laser power such that the output dc level I_R is just below the saturation threshold of the detector. 10kPa noise equivalent pressures (over a 25MHz measurement bandwidth), comparable to PVDF transducers are readily achieved with such a configuration^{12,14}. To improve upon this requires the design of a high finesse cavity to “sharpen” the transfer function. At least an order of magnitude increase in sensitivity should be possible albeit with a reduced upper limit of linear detection. Additionally, an increased wavelength tuning range is required in order to avoid the 2π radians of “dead space” between the resonant peaks of ITF where sensitivity is zero. Higher wavelength stability is also necessary to hold the system at the optimum phase bias.

3.3 Frequency response

For a sensing film of sufficiently large lateral dimensions, radial resonance modes and the effects of acoustic diffraction at the boundaries of the film can be neglected. The sensor is then said to operate in thickness mode. The frequency response $P_I(k)$ depends upon the spatial variation of acoustic pressure P_T due to the incident acoustic wave and its reflection within the film arising from the acoustic impedance mismatch at its boundaries. $P_I(k)$ is obtained by evaluating the mean distribution of stress across the thickness l of the film as a function of frequency¹²

$$P_I(k) = \frac{1}{l} \int_l P_T dx \quad (3)$$

where k is the acoustic wavenumber. The thickness of the sensing film in relation to the acoustic wavelength determines the bandwidth. The acoustic impedance mismatches at the boundaries of the film, on one side due to the backing, on the other due to water determines the uniformity of response. In general, polymer films have an acoustic impedance close to water and the uniform broadband response characteristics of a low Q system can be expected.

Figure 3 shows the experimentally measured frequency response of three physically useful configurations. In each case 50 μ m thick PET sensing films were used. The water backed configuration shows the small $\lambda/2$ thickness mode resonance (at ~20MHz) characteristic of a water backed polymer film – a similar response can be observed with PVDF membrane hydrophones. For the glass backed sensing film, which approximates to a rigid backed configuration, ($|P(k)|=2$) and the bandwidth is reduced by a factor of 2 with a $\lambda/4$ resonance at approximately 9MHz. The resonance is at a slightly lower frequency than it should be due to bandlimiting effect of the adhesive layer (~1.5 μ m) between the sensing film and glass backing. In the PMMA-backed configuration, the acoustic impedance of the PET sensing film, adhesive layer and PMMA backing are very similar (~3 x 10⁶ Kg/m²s). Thus there is no resonance and the response rolls off with increasing frequency.

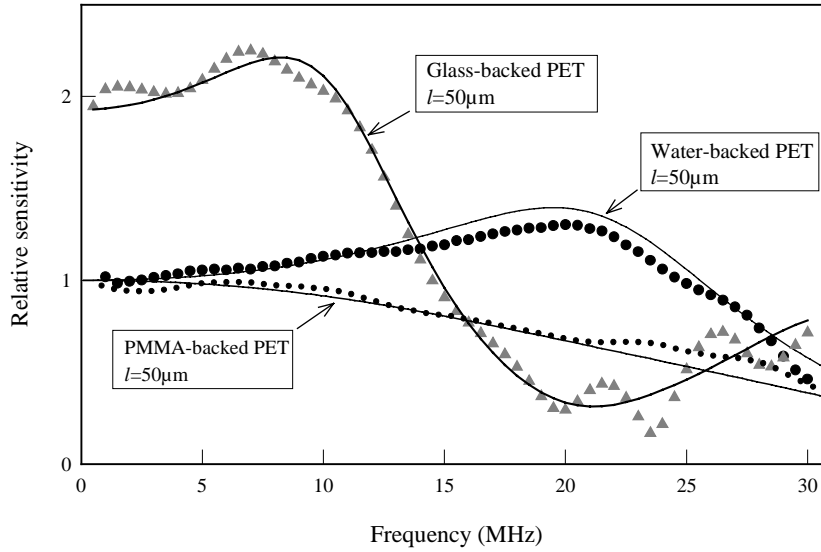


Figure 3 Experimentally measured frequency responses of three different backing configuration using $50\mu\text{m}$ PET sensing film. The continuous lines show the predicted response calculated using equation 3.

3.4 Effective element size

The effective element size is a measure of the acoustic aperture of a receiver. Its effect on lateral spatial resolution makes it a key parameter in an ultrasonic imaging system. It is of particular importance in phased array systems where the requirement is for each element to have a near isotropic directional response requiring the element size to be small in relation to the acoustic wavelength. To a first approximation, the element size of the FP polymer film sensing concept is defined by the dimensions of the optical field addressing the film. Thus, in principal, element sizes down to the optical diffraction limit of a few microns are feasible offering the prospect of an omnidirectional response at acoustic frequencies as high as 50MHz. This can be achieved without compromising sensitivity as, unlike piezoelectric transducers, sensitivity is independent of element size for a given optical intensity.

Clearly there will be a limit to the assumption that the active area is defined only by the region that is optically addressed.. Acoustically-induced thickness deformations outside the optically defined area of an “element” will, to some extent, contribute to its output increasing the acoustic aperture. This effect can be assessed by measuring the directional response of the element as a function of acoustic frequency. By fitting the first order Bessel function of the angular response of a circular plane piston in a rigid baffle¹⁵ to the experimental data, the effective radii at each frequency can be determined. This has been studied in a previous paper¹⁴ by illuminating a polymer sensing film with the output of a $6\mu\text{m}$ core diameter single mode optical fibre. Directivity measurements at several frequencies are shown in figure 4(a) illustrating low directional sensitivity to 10MHz. The corresponding effective radii at 1MHz intervals to 10MHz are shown in figure 4(b). In common with piezoelectric PVDF receivers, the effective radii falls off with frequency¹⁴. This is thought to be due to the apodised response of the sensor arising from the Gaussian profile of the output of the single mode optical fibre. Beyond 10MHz, where the effective radii (not shown in fig 4(b)) would be expected to level out a value close to optically defined element size, the effects of acoustic diffraction around the tip of the fibre were found to distort the directivity plots making it impossible to recover the effective radius. Thus it is difficult to say categorically what eventual minimum effective radius would be. However, from the measurements *below* 10MHz the effective radius is (at worst) estimated at $35\mu\text{m}$ and is quite possibly significantly lower.

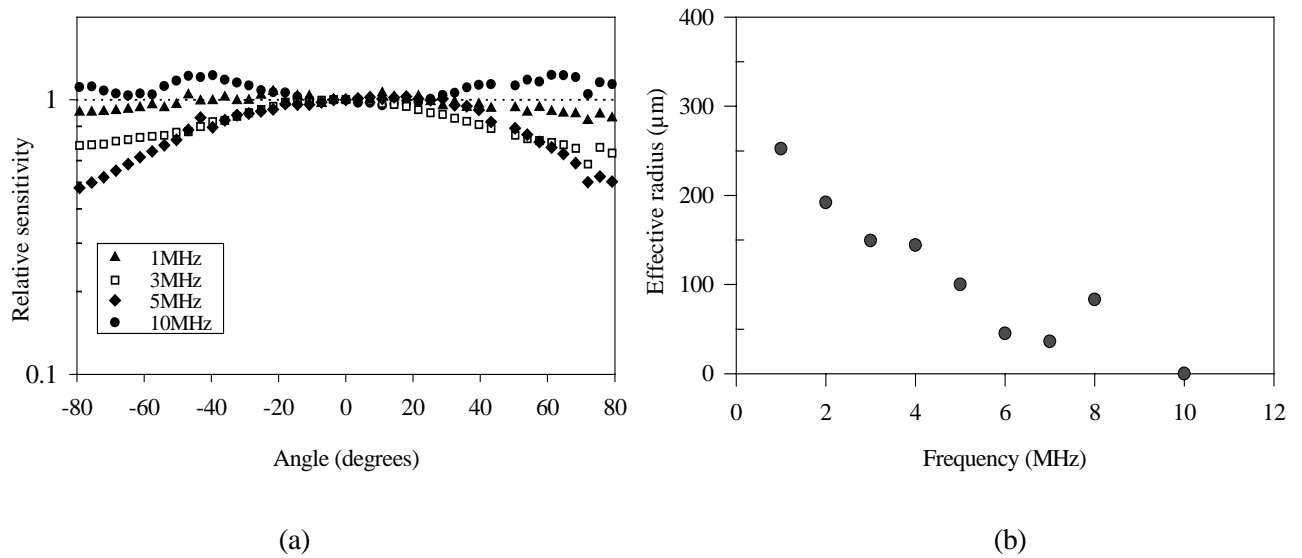


Figure 4 (a) Directional response of FP polymer film transducer illuminated with the output of a $6\mu\text{m}$ core single mode optical fibre, (b) Effective radius as a function of frequency.

4. PROTOTYPE IMAGING SENSOR HEAD

To test the concept outlined in section 2 a prototype sensor head was fabricated. A schematic is shown in figure 5. For simplicity, aluminium coatings were used to provide the mirrors of the FP cavity. Thus the sensor head was not transparent to excitation laser pulses and acted only a receiving array. The glass backing stub was first coated with a partially reflective aluminium coating. A $50\mu\text{m}$, thick polymer film (Parylene) was deposited followed by a second, fully opaque aluminium coating. A wedge was formed on the optical input side of the sensor head to eliminate parasitic interference between the light reflected from the sensing film and that from the front face of the glass backing stub.

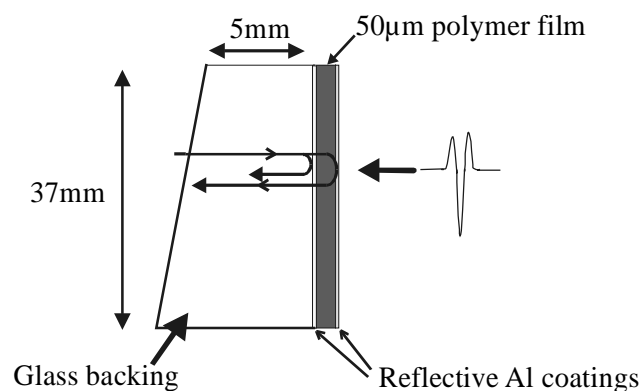


Figure 5 Prototype imaging sensor head. (37mm x 25mm)

4.1 Characterisation

The bandwidth, linearity and effective radii of the sensor head can reasonably be inferred from previous work^{12,14}. The sensitivity and degree of uniformity of sensitivity over the sensor head were therefore considered to be the key parameters to be measured. The latter is of particular importance as it provides an indication of the level of signal processing required to interrogate the sensor head. The principal source of variations in sensitivity is likely to be due to changes in the optical thickness across the polymer film. In the worst case, this could necessitate retuning the laser source to return the phase bias to the optimal quadrature point (see figure 2(b)) for each pixel of an image. To investigate this, the experimental scanning set-up shown in figure 6 was set-up. It consists of a 2D computer controlled scanning system which is used to translate the sensor head. A 3.5MHz pulsed piezoelectric transducer held in a fixed position provides a source of ultrasound. The output of a 850nm DBR laser diode is focussed on to the sensor head ($\sim 60\mu\text{m}$ spot size) and the sensor output directed on to a 25MHz photodiode. By scanning the sensor head in two dimensions and monitoring simultaneously the dc optical output of the sensor and its response to the 3.5MHz ultrasound signal, a 2D map of both the reflected interference fringes and the sensitivity across the sensing film were obtained.

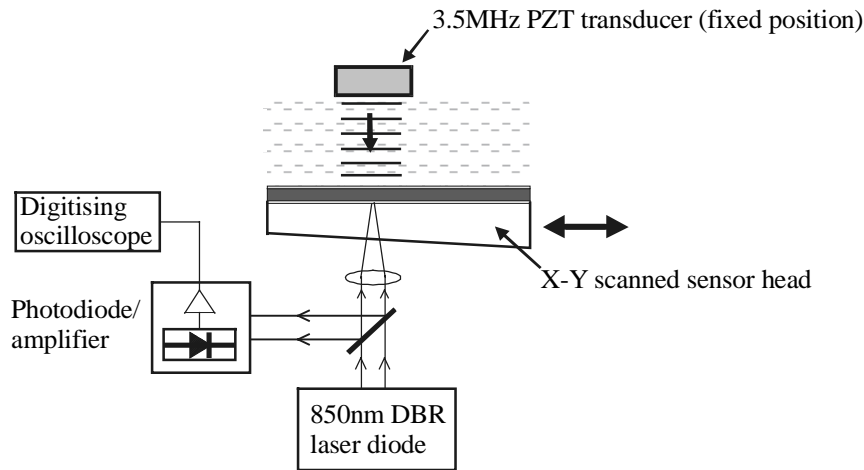


Figure 6 Experimental set-up for sensitivity and fringe mapping.

4.1.1 Sensitivity

The output of the 3.5MHz transducer as measured by the sensor is shown in figure 7. From measurements using a calibrated PVDF membrane hydrophone the sensitivity is estimated to be 100mv/MPa. The peak noise equivalent pressure was 10kPa over a 25MHz measurement bandwidth without signal averaging. An estimate of the interferometer transfer function was obtained from the data displayed in figure 8. This indicated that the sensor was acting as a low finesse FP cavity with a fringe visibility of 0.58. This low value for the visibility is due to the non-optimal reflectivity of the partially reflective aluminium coating. By optimising the reflection coefficient, it should be possible to obtain a factor of two improvement in sensitivity whilst still retaining a low finesse configuration.

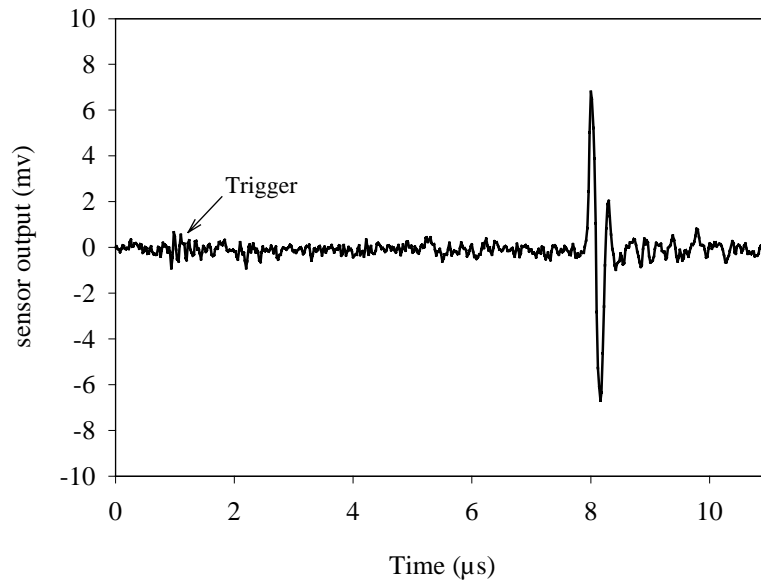


Figure 7 Sensor output due to 3.5MHz signal from PZT transducer

4.1.2 Uniformity of sensitivity

Figure 8(a) shows the reflected dc intensity measured across the sensor head at 300 μ m intervals over a 37 x 25mm area with a 60 μ m spot size. Interference fringes can be seen with two maxima clearly observable indicating a change in optical thickness of 425nm over approximately 20mm. Figure 8(b) shows the corresponding sensitivity map which represent the amplitude of the sensor output due to the 3.5MHz acoustic signal at each point across the sensor head. As expected the sensitivity falls to zero at the positions corresponding to the intensity maxima and minima observed in figure 8(b).

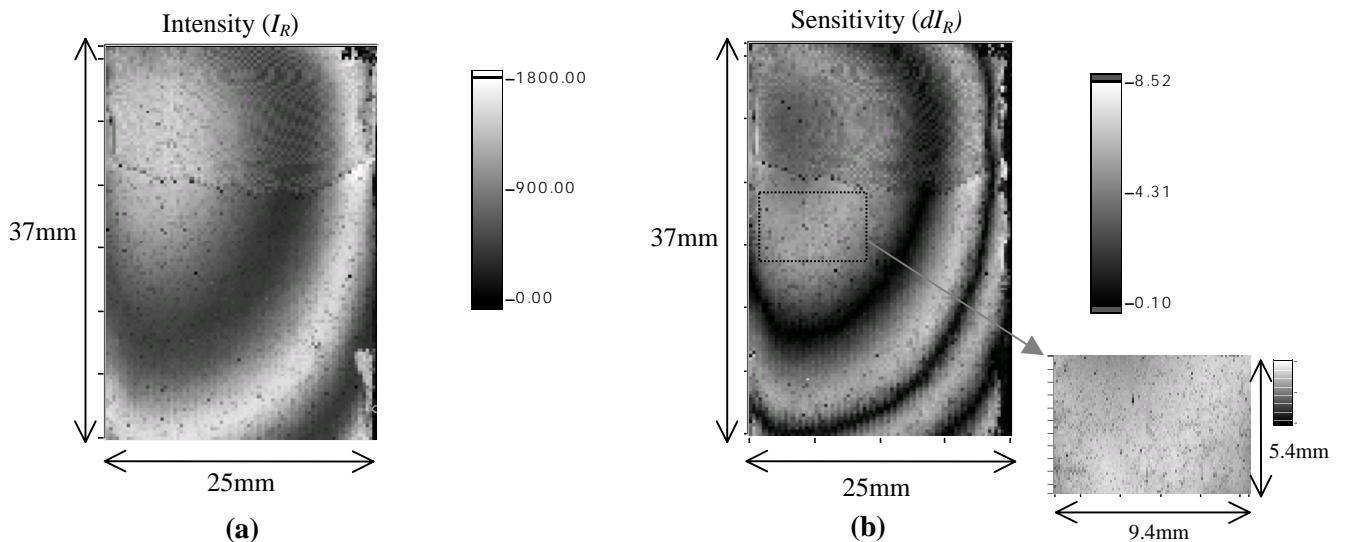


Figure 8 (a) Reflected interference fringes across sensor head and (b) corresponding sensitivity map. 60 μ m spot size, 300 μ m steps. Dotted area on sensitivity map shows location of region of uniform sensitivity – rescanned with 100 μ m steps.

There are two approaches to dealing with variations in sensitivity across the sensor head. The first is to select a region as shown in figure 8(b) where the variations are acceptably small and limit detection to this area only. To obtain a larger sensing area, a more practical approach is to shift the interference fringes and hence the sensitivity distribution across the sensor head by tuning the laser wavelength. By adjusting the phase bias in this way, optimum sensitivity can be obtained at each point.

5. CONCLUSIONS

The feasibility of a 2D ultrasound array based upon the FP polymer film sensing concept for photoacoustic imaging has been discussed. Uniform wideband frequency response to 20 MHz, effective element sizes of $<35\mu\text{m}$ and kPa acoustic pressure resolutions suggest that the concept has excellent potential as an alternative to piezoelectric detection methods for photoacoustic imaging. A prototype imaging sensor head has been fabricated and the variation of sensitivity due to changes in optical thickness across the polymer sensing film have been assessed. Small areas ($<1\text{cm}^2$) of adequately uniform sensitivity can be identified which may be useful for demonstrating the concept for photoacoustic imaging. For a practical system however, some form of active phase bias control is likely to be necessary. Future work is to concentrate on this and the development of a sensing head that is transparent to the excitation laser pulses for backward-mode photoacoustic imaging.

6. REFERENCES

- ¹ Kruger RA, Kopecky KK, Aisen AM, Reinecke DR, Kruger GA, Kiser WL, Thermoacoustic CT with Radio Waves: A Medical Imaging Paradigm, *Radiology*, Vol. 211, No. 1, pp275-278, 1999
- ² Oraevsky AA, Andreev VA, Karabutov AA, Fleming DR, Gatalica Z, Singh H, Esenaliev R, Laser opto acoustic imaging of the breast: detection of cancer angiogenesis, *SPIE Vol 3597*, pp352-363, 1999
- ³ Oraevsky AA, Karabutov AA, Savateeva EB, Bell B, Motamedi M, Thomsen SL, Pasricha P, Opto-acoustic imaging of oral cancer: feasibility studies in hamster model of squamous cell carcinoma, *SPIE Vol 3597*, pp385-396, 1999
- ⁴ Hoelen CG, de Mul FFM, Pongers R, Dekker A, , Three-dimensional photoacoustic imaging of blood vessels in tissue, *Optics Letters*, Vol 23, No 8, pp648-650, 1998
- ⁵ Hoelen CGA, Kolkman RGM, Letteboer M, Berendsen R, De Mul FFM, Photoacoustic tissue scanning, *Proc SPIE*, Vol 3597, pp336-343, 1999
- ⁶ Beard PC and Mills T.N, Characterisation of *post mortem* arterial tissue using time-resolved photoacoustic spectroscopy at 436nm, 461nm and 532nm, *Physics in Medicine and Biology*, Vol 42, No 1, pp177-198, 1997
- ⁷ Paltauf G. and Schmidt-Kloiber H., Measurement of laser-induced acoustic waves with a calibrated optical transducer, *J. Appl. Phys.*, **82** (4), pp1525-1531, 1997
- ⁸ Paltauf G., Schmidt-Kloiber and Guss H., Light distribution measurements in absorbing materials by optical detection of laser induced stress waves, *Appl. Phys. Lett.*, 69 (11), pp 1526-1528, 1996
- ⁹ Paltauf G and Schmidt-Kloiber H, Optical method for two dimensional ultrasonic detection, *Applied Physics Letters*, Vol 75, No 8, pp1048-1050, 1999
- ¹⁰ Hamilton JD and O'Donnell M, High frequency ultrasound imaging with optical arrays, *IEEE Transactions on Ultrasonics, Ferroelectrics and Frequency Control*, Vol 45, No 1, pp216-235, 1998
- ¹¹ Wilkens V. and Koch Ch., Optical multilayer detection array for fast ultrasonic field mapping, *Optics Letters*, Vol 24, No 15, pp1026-1028, 1999
- ¹² Beard PC, Perennes F, Mills TN, Transduction mechanisms of the Fabry Perot polymer film sensing concept for wideband ultrasound detection., *IEEE Transactions on Ultrasonics, Ferroelectrics and Frequency control*, Vol 46, No 6, pp1575-1582, 1999
- ¹³ Beard PC, Perennes F, Dragioti E, Mills TN, An optical fibre photoacoustic-photothermal probe, *Optics Letters*, Volume 23, Issue 15, pp. 1235-1237, 1998
- ¹⁴ Beard PC, Hurrell A, Mills TN, Characterisation of a polymer film optical fibre hydrophone for the measurement of ultrasound fields for use in the range 1-30MHz: a comparison with PVDF needle and membrane hydrophones, *IEEE Transactions on Ultrasonics, Ferroelectrics and Frequency control*, Vol 47, No1, p256-264, 2000
- ¹⁵ Morse PM and Ingard UK, *Theoretical Acoustics* (McGraw-Hill, New York), p381, 1968